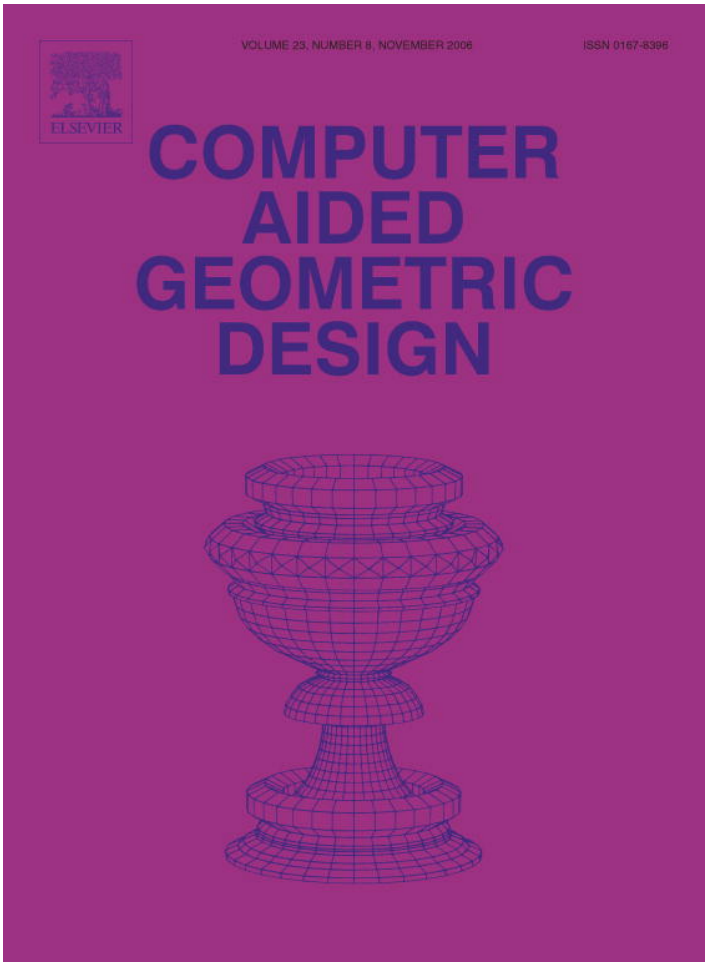

Available online at www.sciencedirect.com
ScienceDirect
Computer Aided Geometric Design 23 (2006) 640–654
COMPUTER AIDED GEOMETRIC DESIGN
www.elsevier.com/locate/cagd

An octahedral C^2 macro-element ☆

Ming-Jun Lai [a], Alan Le Méhauté [b], Tatyana Sorokina [a,*]

[a] *Department of Mathematics, The University of Georgia, Athens, GA 30602, USA*
[b] *Department of Mathematics, The University of Nantes, F.44322 Nantes, France*

Received 12 May 2005; received in revised form 12 June 2006; accepted 14 June 2006

Available online 14 July 2006

Abstract

A macro-element of smoothness C^2 is constructed on the split of an octahedron into eight tetrahedra. This new element complements those recently constructed on the Clough–Tocher and Worsey–Farin splits of a tetrahedron (cf. Alfeld, P., Schumaker, L.L., 2005a, 2005b). The octahedral element uses supersplines of degree thirteen, and provides optimal order of approximation of smooth functions.

MSC: 41A15; 65M60; 65N30

Keywords: Macro-elements; Spline spaces; Octahedron

1. Introduction

This paper is designed to compliment two recent results on trivariate C^2 macro-elements obtained by P. Alfeld and L.L. Schumaker. The first one, constructed in (Alfeld and Schumaker, 2005a), is based on the three-dimensional Clough–Tocher split of a tetrahedron into four subtetrahedra, and uses polynomial splines of degree thirteen. The second macro-element is described in (Alfeld and Schumaker, 2005b), and based on the Worsey–Farin split of a tetrahedron into twelve subtetrahedra. The Worsey–Farin split is more complicated, and allows the use of polynomial splines of degree nine. In our paper, we use the split of an octahedron into eight tetrahedra (for details, see Definition 3.1). Our macro-element uses polynomial splines of the same degree as the Clough–Tocher one, thirteen. Whenever applicable, it has an obvious advantage over the Clough–Tocher macro-element. It does not require the splitting of each tetrahedron into subtetrahedra. Although octahedral partitions of a domain in $\mathbb{R}^3$ are less common than tetrahedral ones, they naturally arise from a number of applications. In particular, uniform type grids are well-suited for using octahedral macro-elements (see Remark 6.3). In contrast to tensor-product splines, macro-elements provide full approximation power. Another important application of octahedral macro-elements comes from the uniform refinement of tetrahedral partitions (see Remark 6.5). Moreover, for some partitions it is possible to use a combination of the 3D Clough–Tocher macro-element and our octahedral element (see Remarks 6.4 and 6.6).

☆ Results in this paper are based on the research supported by the National Science Foundation under the grant No. 0327577.
* Corresponding author.
E-mail addresses: mjlai@math.uga.edu (M.-J. Lai), alm@math.univ-nantes.fr (A. Le Méhauté), sorokina@math.uga.edu (T. Sorokina).

0167-8396/$ – see front matter
doi:10.1016/j.cagd.2006.06.001

Following (Alfeld and Schumaker, 2005a), we define a *trivariate macro-element on an octahedron* P as a pair $(\mathcal{S}, \Lambda)$, where $\mathcal{S}$ is a space of polynomial splines defined on a partition of P into tetrahedra, and Λ is a set of linear functionals consisting of values and derivatives of $s \in \mathcal{S}$ at some points in P, that uniquely define s. Let $\triangle$ be an octahedral partition of a polygonal domain $\Omega \subset \mathbb{R}^3$, such that if two octahedra intersect at a vertex, edge, or face, then they share this vertex, edge, or face, respectively. We say that a macro-element has *smoothness* C^2 if the macro-element used on each octahedron results in a globally C^2 continuous function.

This paper is organized as follows. In Section 2 we review some basic Bernstein–Bézier techniques for spline functions over tetrahedral partitions and introduce new notation for later use. Section 3 contains the description of our split of an octahedron and several facts about the location of domain points. In Section 4 we describe our C^2 macro-element and obtain error bounds for Hermite interpolation using the octahedral macro-element. We prove several useful bivariate lemmas in Section 5 which are needed for the proof of the main result in Section 4. The paper is concluded with several remarks in Section 6.

2. Preliminaries

Let $\triangle$ be a tetrahedral partition of a polyhedral domain Ω in $\mathbb{R}^3$. We define the set of polynomial splines of degree d and smoothness r on $\triangle$ as

$$\mathcal{S}_d^r(\triangle) := \big\{ s \in C^r(\Omega) \colon\ s|_T \in \mathcal{P}_d^3,\ \text{for all tetrahedra } T \in \triangle \big\},$$

where $\mathcal{P}_d^3$ is the space of trivariate polynomials of degree d. We use Bernstein–Bézier techniques as in (Alfeld and Schumaker, 2002a, 2002b; Lai and Schumaker, 2001, 2003). In particular, given a tetrahedron $T := \langle v, u, w, t \rangle$, we represent a polynomial p of degree d in its B-form with respect to T:

$$p = \sum_{i+j+k+l=d} c_{ijkl}^T B_{ijkl}^d,$$

where B_{ijkl}^d are the *Bernstein polynomials* of degree d associated with T. As usual, we associate the coefficients c_{ijkl}^T with the *domain points*

$$\mathcal{D}_{T,d} := \left\{ \xi_{ijk}^T := \frac{iv + ju + kw + lt}{d},\ i + j + k + l = d \right\}. \tag{2.1}$$

Fig. 1 (left) shows all domain points in $\mathcal{D}_{T,5}$. Let $\mathcal{S}_d^0(\triangle)$ be the space of continuous splines of degree d on $\triangle$, and let $\mathcal{D}_{\triangle,d}$ be the union of the sets of domain points associated with each tetrahedron of $\triangle$. Then it is well known that each spline in $\mathcal{S}_d^0(\triangle)$ is uniquely determined by its set of B-coefficients $\{c_\xi\}_{\xi \in \mathcal{D}_{\triangle,d}}$, where the coefficients of the polynomial $s|_T$ are precisely $\{c_\xi\}_{\xi \in \mathcal{D}_{T,d}}$.

If v is a vertex of a tetrahedron $T = \langle v, u, w, t \rangle$, then we define the *shell of radius m around v in T* as

$$H_m^T(v) := \big\{ \xi_{d-m,j,k,l}^T \in \mathcal{D}_{T,d},\ \text{for all } j + k + l = m \big\}. \tag{2.2}$$

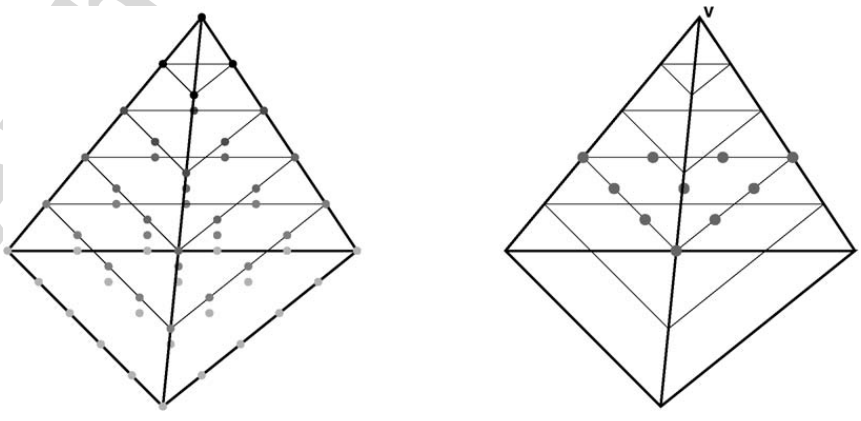

Fig. 1. Domain points in $\mathcal{D}_{T,5}$ (left) and $H_3^T(v) \cap \mathcal{D}_{T,5}$ (right).

Fig. 1 (right) shows $H_3^T(v) \cap \mathcal{D}_{T,5}$. The *ball of radius m around v in T* is defined as

$$B_m^T(v) := \bigcup_{i=0}^{m} H_i^T(v). \tag{2.3}$$

We define the *frame of the shell* $H_m^T(v)$ as

$$Fr\big(H_m^T(v)\big) := \big\{\xi_{ijkl}^T \in H_m^T(v), \text{ for all } j \times k \times l = 0\big\}. \tag{2.4}$$

The *tube of radius m around the edge* $\langle v, u\rangle$ *in T* is

$$E_m^T\big(\langle v, u\rangle\big) := \big\{\xi_{ijkl}^T \in \mathcal{D}_{T,d}, \text{ for all } k + l \leqslant m, \text{ and } i + j = d - k - l\big\}. \tag{2.5}$$

We also need to define the *p-ball of radius m around v in T*:

$$B_{\otimes,m}^T(v) := \big\{\xi_{ijkl}^T \in \mathcal{D}_{T,d}, \text{ for all } i + j + k + l = d, \text{ with } \max\{j, k, l\} \leqslant m\big\}. \tag{2.6}$$

Fig. 2 illustrates the visible surface of $B_{\otimes,3}^T(t) \cap \mathcal{D}_{T,13}$. The domain points on the surface of the p-ball are located at the intersections of the line segments on the three visible faces of the box.

In general, if v is a vertex of a tetrahedral partition $\triangle$, we define the *shell* $H_m(v)$ *of radius m around v* as

$$H_m(v) := \big\{H_m^T(v), \text{ for all } T := \langle v, u, w, t\rangle \text{ sharing } v \text{ in } \triangle\big\}, \tag{2.7}$$

where each domain point is counted once if it belongs to more than one tetrahedra in $\triangle$.

The *ball* $B_m(v)$, *frame* $Fr(H_m(v))$, *tube* $E_m(\langle v, u\rangle)$, *and p-ball* $B_{\otimes,m}(v)$ *of radius m around v* are defined similarly.

Additionally, we recall that in the bivariate setting, if v is a vertex of a triangulation $\triangle$, and $\mathcal{D}_{\triangle,d}$ is the set of domain points for $s \in \mathcal{S}_d^0(\triangle)$, then the *ring* $R_m(v)$ *of radius m around v* is defined as

$$R_m(v) := \big\{\xi_{d-m,i,j}^T \in \mathcal{D}_{\triangle,d}, \text{ for all triangles } T := \langle v, u, w\rangle \in \triangle, \text{ for all } i + j = m\big\}. \tag{2.8}$$

The *disk* $D_m(v)$ *of radius m around v* is

$$D_m(v) := \bigcup_{i=0}^{m} R_i(v). \tag{2.9}$$

We shall use these notions in Section 5.

Given a multi-index $\alpha = (\alpha_1, \alpha_2, \alpha_3)$ with nonnegative integer entries, we define

$$|\alpha| := \alpha_1 + \alpha_2 + \alpha_3, \qquad \|\alpha\| := \max\{\alpha_1, \alpha_2, \alpha_3\}. \tag{2.10}$$

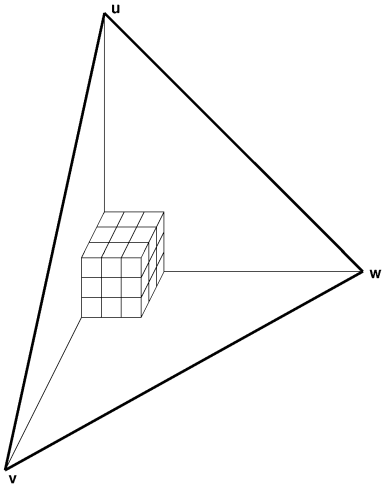

Fig. 2. The visible surface of the p-ball of radius 3 around t in $T = \langle v, u, w, t\rangle$.

We write D^α for the partial derivative $D_x^{\alpha_1} D_y^{\alpha_2} D_z^{\alpha_3}$. Given an edge $e := \langle u, v\rangle$ of a tetrahedron $T \in \triangle$, and a multi-index $\beta = (\beta_1, \beta_2)$, we define D_e^β to be the partial derivative associated with two non-collinear vectors orthogonal to e. That is,

$$D_e^\beta = D_{e_1}^{\beta_1} D_{e_2}^{\beta_2} \tag{2.11}$$

where e_1, e_2 denote two non-collinear vectors that are perpendicular to e. We also need notation for the following points on e:

$$\eta_{e,j}^i := \frac{(i-j+1)u + jv}{i+1}, \quad j = 1, \ldots, i. \tag{2.12}$$

Given a face $F := \langle u, v, w\rangle$ of a tetrahedron $T \in \triangle$, and a nonnegative integer k, we define D_F^k to be the kth order derivative associated with a unit vector orthogonal to F. Finally, if η is a point in $\mathbb{R}^3$, we use ε_η to denote the point-evaluation functional associated with η, i.e., $\varepsilon_\eta := f(\eta)$.

As is well known, a spline $s \in \mathcal{S}_d^0(\triangle)$ will belong to $C^2(\Omega)$ if and only if certain smoothness conditions across faces between adjoining tetrahedra are satisfied. To describe these in B-form instead of usual derivatives, suppose that $T := \langle v_1, v_2, v_3, v_4\rangle$ and $\widetilde{T} := \langle v_5, v_2, v_3, v_4\rangle$ are two adjoining tetrahedra sharing a face $F := \langle v_2, v_3, v_4\rangle$. Suppose

$$s|_T = \sum_{i+j+k+l=d} c_{ijkl}^T B_{ijkl}^d, \quad \text{and} \quad s|_{\widetilde{T}} = \sum_{i+j+k+l=d} c_{ijkl}^{\widetilde{T}} \widetilde{B}_{ijkl}^d,$$

where $\{\widetilde{B}_{ijkl}^d\}_{i+j+k+l=d}$ are the Bernstein polynomials of degree d associated with $\widetilde{T}$. Given $1 \leqslant i \leqslant d$, let

$$\tau_{jkl}^i := c_{ijkl}^T - \sum_{\nu+\mu+\kappa+\ell=i} c_{\nu,j+\mu,k+\kappa,l+\ell}^{\widetilde{T}} \widetilde{B}_{\nu\mu\kappa\ell}^i(v_1) \tag{2.13}$$

for all $j + k + l = d - i$. Following (Alfeld and Schumaker, 2002a), we call τ_{jkl}^i a *smoothness functional of order* i. Note that for a given pair of adjoining tetrahedra, this functional is uniquely associated with the domain point $\xi_{ijkl}^T \in \mathcal{D}_{T,d}$. In order to identify such a functional we need to specify T, $\widetilde{T}$, and F. We use the following notation

$$\left\{\tau_{jkl}^i, (v_a, \langle v_b, v_c, v_d\rangle, v_e)\right\} \tag{2.14}$$

to describe the smoothness functional of order i, associated with the point ξ_{ijkl} in $T := \langle v_a, v_b, v_c, v_d\rangle$ across the face $F := \langle v_b, v_c, v_d\rangle$ shared by the neighboring tetrahedron $\widetilde{T} := \langle v_e, v_b, v_c, v_d\rangle$. It is well known that a spline $s \in \mathcal{S}_d^0(\triangle)$ is C^r continuous across the face F, for $1 \leqslant r \leqslant d$, if and only if

$$\tau_{jkl}^i s = 0, \quad \text{for all } j + k + l = d - i,\ i = 1, \ldots, r.$$

We will also use bivariate smoothness functionals. They are defined similarly to (2.13). In order to identify a bivariate smoothness functional we need to specify a triangle F, the neighboring triangle $\widetilde{F}$, and the edge e that they share. We use the following notation

$$\left\{\tau_{jk}^i, (v_a, \langle v_b, v_c\rangle, v_d)\right\} \tag{2.15}$$

to describe the smoothness functional of order i, associated with the point ξ_{ijk} in $F := \langle v_a, v_b, v_c\rangle$ across the edge $e := \langle v_b, v_c\rangle$ shared by the neighboring triangle $\widetilde{F} := \langle v_d, v_b, v_c\rangle$.

Given a vertex v of $\triangle$, and $1 \leqslant r \leqslant d$, we say that $s \in C_\otimes^r(v)$, if for all $T \in \triangle$ attached to v, the values of $D^\alpha|_T(v)$ coincide, $\|\alpha\| \leqslant r$.

Suppose $\mathcal{S}$ is a linear subspace of $\mathcal{S}_d^0$, and $\mathcal{M} \subset \mathcal{D}_{\triangle,d}$. Then $\mathcal{M}$ is *a determining set for* $\mathcal{S}$ provided that if $s \in \mathcal{S}$ and its B-coefficients satisfy $c_\xi = 0$ for all $\xi \in \mathcal{M}$, then $s \equiv 0$. The set $\mathcal{M}$ is called *a minimal determining set* (*MDS*) *for* $\mathcal{S}$ provided that there is no smaller determining set.

Suppose $\mathcal{N}$ is a set of linear functionals λ (usually defined as point-evaluations of values or derivatives of s). Then $\mathcal{N}$ is *a nodal determining set for* $\mathcal{S}$ provided that if $s \in \mathcal{S}$ and $\lambda s = 0$ for all $\lambda \in \mathcal{N}$, then $s \equiv 0$. The set $\mathcal{N}$ is called *a nodal minimal determining set* (*NMDS*) *for* $\mathcal{S}$ provided that there is no smaller nodal determining set.

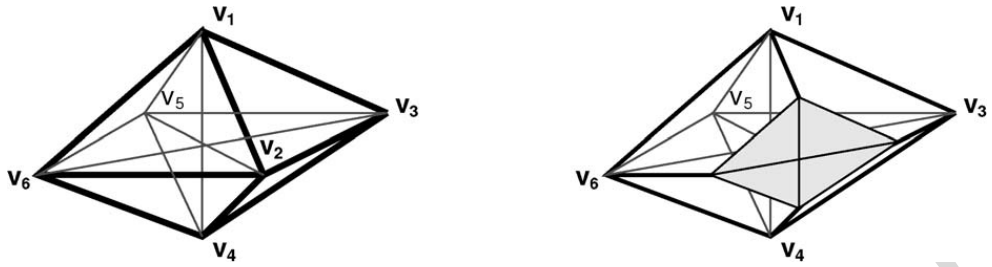

Fig. 3. The split of the octahedron (left) and the cross-section associated with shells around v_2 (right).

3. The split of the octahedron and subsets of domain points

By drawing three not coplanar lines through any point O in $\mathbb{R}^3$ we obtain a *cross* in $\mathbb{R}^3$. Two points v_i and v_j on each line are chosen so that O is inside of the segment (v_i, v_j). The convex hull of these six vertices forms a cross polytope P. We call such a cross polytope an octahedron. That is, we require that all three diagonals of an octahedron intersect at one point.

Definition 3.1. Given an octahedron $P = \{v_1, v_2, v_3, v_4, v_5, v_6\}$, let O_P be the intersection of its three diagonals: $\langle v_1, v_4\rangle, \langle v_2, v_5\rangle, \langle v_3, v_6\rangle$, as shown in Fig. 3 (left). Draw in the line segments $\langle v_i, O_P\rangle$, $i = 1, \ldots, 6$. The resulting partition of P into eight tetrahedra is called $\triangle_P$, see Fig. 3 (left).

We write $\mathcal{V}_P$, $\mathcal{E}_P$, and $\mathcal{F}_P$ for the sets of six vertices, twelve edges, and eight faces of P, respectively. By $\mathcal{D}_{\triangle_P,13}$ we denote the set of domain points for $s \in \mathcal{S}_{13}^0(\triangle_P)$. In the remainder of this section we prove several lemmas which are needed for the proof of the main result of Section 4.

Lemma 3.2. *Let u and v be two vertices of P connected by the edge $e := \langle u, v\rangle$. The intersection of the shells of radius r around u and radius t around v is contained in the tube of radius four around e for all $r, t \in \{4, \ldots, 9\}$, except $(r, t) = (9, 9)$.*

Proof. First we observe that $H_r(u) \cap H_t(v)$ lies in two tetrahedra $T := \langle O_P, w, u, v\rangle$ and $\widetilde{T} := \langle O_P, \tilde{w}, u, v\rangle$. Due to symmetry, it suffices to consider $H_r(u) \cap H_t(v)$ in T. By definition (2.2)

$$H_r^T(u) = \big\{\xi^T_{i,j,13-r,k},\ i + j + k = r\big\}, \qquad H_t^T(v) = \big\{\xi^T_{m,n,l,13-t},\ m + n + l = t\big\}.$$

Then

$$H_r^T(u) \cap H_t^T(v) = \big\{\xi^T_{i,j,13-r,13-t},\ i + j = r + t - 13\big\}. \tag{3.1}$$

For $r, t \in \{4, \ldots, 9\}$, $(r, t) \neq (9, 9)$, the maximal value of the sum $r + t - 13$ is equal to 4. Therefore, by (2.5), the points in (3.1) belong to $T_4(e)$. □

We also need a very detailed description of the intersection of the shells of radius nine of two neighboring vertices of P.

Lemma 3.3. *Let u and v be two vertices of P connected by the edge $e := \langle u, v\rangle$, and $T_e := \langle w, O_P, u, v\rangle$, $\widetilde{T}_e := \langle \tilde{w}, O_P, u, v\rangle$ be the two tetrahedra in $\triangle_P$ sharing e. Let $\mathcal{M}_e$ be the intersection of shells of radius nine around u and v. Then*

$$\mathcal{M}_e := \big\{\xi^{T_e}_{5044}, \xi^{T_e}_{4144}, \xi^{T_e}_{3244}, \xi^{T_e}_{2344}, \xi^{T_e}_{1444}, \xi^{T_e}_{0544}, \xi^{\widetilde{T}_e}_{1444}, \xi^{\widetilde{T}_e}_{2344}, \xi^{\widetilde{T}_e}_{3244}, \xi^{\widetilde{T}_e}_{4144}, \xi^{\widetilde{T}_e}_{5044}\big\}. \tag{3.2}$$

Moreover, $\mathcal{M}_e$ can be decomposed into the following two subsets:

$$\mathcal{M}_e^1 := \big\{\xi^{T_e}_{5044}, \xi^{T_e}_{4144}, \xi^{T_e}_{3244}, \xi^{\widetilde{T}_e}_{3244}, \xi^{\widetilde{T}_e}_{4144}, \xi^{\widetilde{T}_e}_{5044}\big\} \subset \big\{H_{13}(O_P) \cup H_{12}(O_P) \cup H_{11}(O_P)\big\},$$
$$\mathcal{M}_e^2 := \big\{\xi^{T_e}_{2344}, \xi^{T_e}_{1444}, \xi^{T_e}_{0544}, \xi^{\widetilde{T}_e}_{1444}, \xi^{\widetilde{T}_e}_{2344}\big\} \subset \big\{H_{10}(O_P) \cup H_9(O_P) \cup Fr\big(H_8(O_P)\big)\big\},$$

and

$$\mathcal{M}_e^2 \cap \big\{B_6(t) \cup E_4(b) \cup B_6(O_P) \cup B_{\otimes,3}(O_P)\big\} = \emptyset, \quad \textit{for any } t \in \mathcal{V}_P,\ b \in \mathcal{E}_P.$$

Proof. Using definition (2.2) we see that

$$H_9^{T_e}(u) = \big\{\xi^{T_e}_{i,j,4,k},\ i+j+k=9\big\}, \qquad H_9^{T_e}(v) = \big\{\xi^{T_e}_{m,n,l,4},\ m+n+l=9\big\}.$$

Thus,

$$H_9^{T_e}(u) \cap H_9^{T_e}(v) = \big\{\xi^{T_e}_{i,j,4,4},\ i+j=5\big\}.$$

By symmetry

$$H_9^{\widetilde{T}_e}(u) \cap H_9^{\widetilde{T}_e}(v) = \big\{\xi^{\widetilde{T}_e}_{i,j,4,4},\ i+j=5\big\}.$$

Next, we observe that $\xi^{T_e}_{0544}$ coincides with $\xi^{\widetilde{T}_e}_{0544}$, and (3.2) follows. In Fig. 9 (right), the black dots correspond to the domain points in $\mathcal{M}_e^1$, and the open dots mark the points in $\mathcal{M}_e^2$. Using (2.2), (2.4) it can be easily seen that

$$\mathcal{M}_e^1 \subset \big\{H_{13}(O_P) \cup H_{12}(O_P) \cup H_{11}(O_P)\big\},$$
$$\mathcal{M}_e^2 \subset \big\{H_{10}(O_P) \cup H_9(O_P) \cup Fr\big(H_8(O_P)\big)\big\}.$$

By observing that $3 < \max\{i,j,k,l\} < 7$ for any $\xi_{ijkl} \in \mathcal{M}_e^2$, and using (2.3), (2.2), and (2.6), we conclude that $\mathcal{M}_e^2$ does not intersect $\{B_6(t) \cup B_6(O_P) \cup B_{\otimes,3}(O_P)\}$ for any $t \in \mathcal{V}_P$. Moreover, since $i+j > 4$ for any $\xi_{ijkl} \in \mathcal{M}_e^2$, the definition of the tube (2.5) implies that $\mathcal{M}_e^2$ has an empty intersection with $E_4(b)$ for any $b \in \mathcal{E}_P$. The proof is now complete. □

Let $\mathcal{M} := \{\mathcal{M}_e\}_{e\in\mathcal{E}_P}$ be the set of pairwise intersections of the shells of radius nine of all six vertices of P. The points forming $\mathcal{M}$ are located on the edges of an extended box (see Fig. 4 (left)). Each edge is described in Lemma 3.3. The three black dots located at the extensions of each corner of the box lie on the faces of P and belong to $H_{13}(O_P)$. They are also shown as black triangles in Fig. 6 (left), and located at the intersections of the line segments on the face $\langle u, v, w\rangle$ in Fig. 4 (right). The black dot at each corner of the box lies on $H_{12}(O_P)$, and actually belongs to the intersection of the shells of radius nine around three neighboring vertices of P. The remaining black dots belong to $H_{11}(O_P)$. The domain points depicted as open dots of a bigger radius lie on the frame of $Fr(H_8(O_P))$. Four of them are shown as open boxes in Fig. 7. The domain points marked as open dots of a smaller radius lie on $H_{10}(O_P) \cup H_9(O_P)$.

The last fact we need is the following lemma.

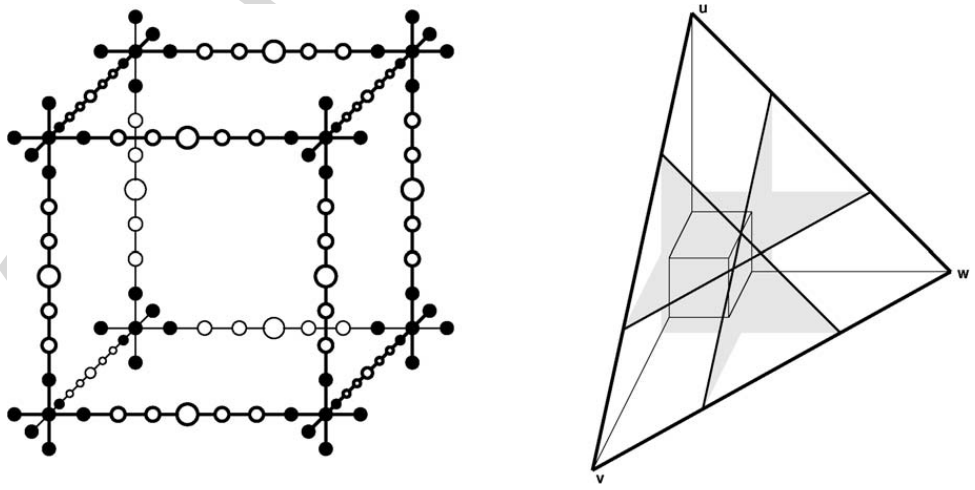

Fig. 4. Pairwise intersections of shells of radius nine around all six vertices of P (left) and one tetrahedron in $\triangle_P$ with the shells of radius nine around u, v, w (right).

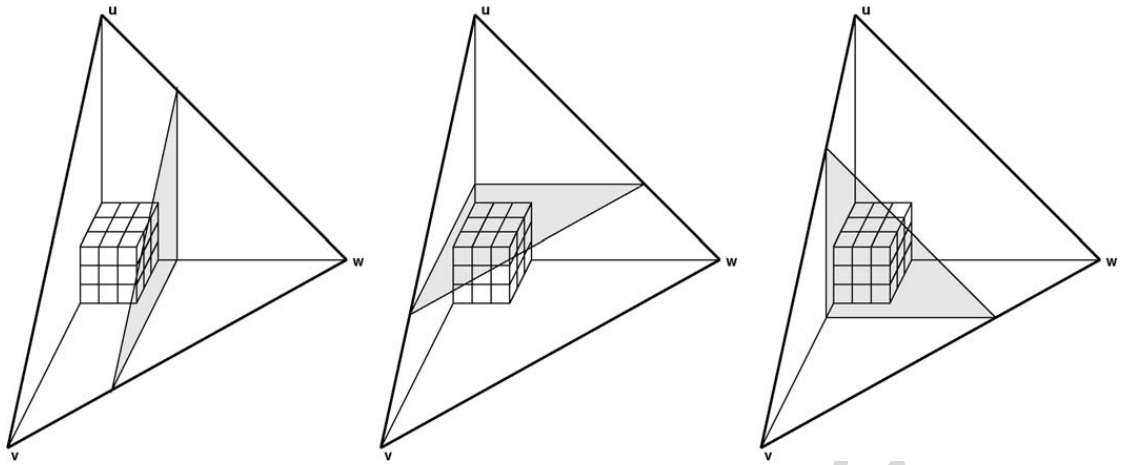

Fig. 5. One tetrahedron in $\triangle_P$ with the p-ball of radius three around O_P and the shell of radius nine around w (left), the shell of radius nine around u (middle) the shell of radius nine around v (right).

Lemma 3.4.

$$\mathcal{D}_{\triangle_P,13} \setminus \{B_9(v)\}_{v\in\mathcal{V}_P} = B_{\otimes,3}(O_P). \tag{3.3}$$

Proof. Let $u, v, w \in \mathcal{V}_P$, and $T := \langle O_P, u, v, w\rangle \in \triangle_P$. Due to symmetry, it suffices to prove (3.3) for domain points in T. By (2.2), $\xi^T_{ijkl} \notin \{B_9(v)\}_{v\in\mathcal{V}_P}$ iff $\max\{j,k,l\} \leqslant 3$. Hence, by (2.6), $\xi^T_{ijkl} \in B_{\otimes,3}(O_P)$. □

Fig. 2 shows the tetrahedron T with $B_{\otimes,3}(O_P)$. Fig. 5 and Fig. 4 (right) illustrate that cutting $B_9(u)$, $B_9(v)$, and $B_9(w)$ off of T does not touch the box $B_{\otimes,3}(O_P)$.

4. An octahedral C^2 macro-element

We would like to precede the definition of the spline space of our interest with a brief discussion to motivate our choice of smoothness conditions and a nodal minimal determining set. First of all, we require the coefficients corresponding to the domain points in $B_6(v)$ for each $v \in \mathcal{V}_P$ have to be set using the value and derivatives at v, cf. the construction in (Alfeld and Schumaker, 2005a). To eliminate some degrees of freedom we also set the coefficients corresponding to the domain points in $B_{\otimes,3}(O_P) \cup B_6(O_P)$ using the value and derivatives at O_P. Next we set the coefficients corresponding to the remaining domain points in $E_3(e)$ for each edge $e \in \mathcal{E}_P$ using derivatives at some points on e. To ensure external C^2 smoothness we also set the coefficients corresponding to the remaining domain points in $H_{13}(O_P) \cup H_{12}(O_P) \cup H_{11}(O_P)$ using the values and derivatives at some points on each $F \in \mathcal{F}_P$.

By Lemma 3.4 the domain points whose coefficients have not been defined from the above are located on $H_i(v)$, $i = 7, 8, 9$, for each $v \in \mathcal{V}_P$. Each shell $H_i(v)$ forms the set of domain points for a bivariate spline of degree i defined on the split of a parallelogram as shown in Fig. 3 (right). To determine unknown coefficients on $H_i(v)$, $i = 7, 8, 9$, we impose additional smoothness conditions on such bivariate splines, see Section 5 for details. However, we have to be careful since the shells around different vertices of P intersect. Lemmas 3.2 and 3.3 describe such intersections.

Now we describe the exact construction of our macro-element. First we introduce special sets of domain points on the triangular faces of P. They are used to construct a nodal determining set. We note that these are the same points as those used in (Alfeld and Schumaker, 2005a). By associating the first index with the vertex O_P of a tetrahedra $T \in \triangle_P$, we place the domain point on a face F of P.

$$\begin{aligned}
\mathcal{A}^0_F &:= \{\xi^T_{0544}, \xi^T_{0454}, \xi^T_{0455}\} = \{\xi^T_{0ijk}\colon i, j, k \geqslant 4\},\\
\mathcal{A}^1_F &:= \{\xi^T_{0ijk}\colon i, j, k \geqslant 3\},\\
\mathcal{A}^2_F &:= \{\xi^T_{0ijk}\colon i, j, k \geqslant 2\} \setminus \{\xi^T_{0272}, \xi^T_{0227}, \xi^T_{0722}\}.
\end{aligned} \tag{4.1}$$

We note that for $i = 2, \ldots, 13$, $v \in \mathcal{V}_P$, the shell $H_i(v)$ forms the set of domain points for a bivariate spline of degree i defined on the split of a two-dimensional cross polytope or parallelogram P^i_v (see the shaded region in

Fig. 3 (right)). We denote such a bivariate spline by s_v^i. Each s_v^i is defined on the split of P_v^i into four subtriangles obtained by drawing in two diagonals of P_v^i.

We now introduce the space of super-splines defined on $\triangle_P$:

$$\begin{aligned}\mathcal{S}_P := \big\{ s \in C^3(P):\ & s|_T \in \mathcal{P}_{13}^3 \text{ all tetrahedra } T \in \triangle_P, \\ & s \in C^6(v) \text{ for all } v \in \mathcal{V}_P,\ s \in C^6(O_P) \cap C^3_{\otimes}(O_P), \\ & \tau_P s = 0 \text{ for all } \tau_P \in \{\mathcal{T}_{e,P},\ e \in \mathcal{E}_P\}, \\ & s_v^i \in S_{P_v^i,i},\ i = 7,8,9 \text{ for all } v \in \mathcal{V}_P \big\}, \end{aligned} \tag{4.2}$$

where for each edge $e := \langle u, v\rangle \in \mathcal{E}_P$, and the two tetrahedra $T := \langle w, O_P, u, v\rangle$, $\widetilde{T} := \langle \tilde{w}, O_P, u, v\rangle$ in $\triangle_P$ attached to e,

$$\mathcal{T}_{e,P} := \big\{ \big\{ \tau_{i44}^{5-i} \big\}, \big(w, \langle O_P, u, v\rangle, \tilde{w}\big),\ i = 0, 1 \big\},$$

and for each $i = 7, 8, 9$, the space of bivariate splines $S_{F,i}$ on the split of a parallelogram F is defined in (5.1)–(5.3).

The smoothness functionals in $\mathcal{T}_{e,P}$ describe individual smoothness conditions of orders five and four across twelve interior faces of $\triangle_P$. Note that they are univariate. The domain points associated with $\{\mathcal{T}_{e,P}\}_{e\in\mathcal{E}_P}$ are depicted in Fig. 4 (left).

Theorem 4.1. *The dimension of the space $\mathcal{S}_P$ is* 1086. *Moreover,*

$$\mathcal{N} := \bigcup_{v\in\mathcal{V}_P} \mathcal{N}_v \cup \bigcup_{e\in\mathcal{E}_P} \mathcal{N}_e \bigcup_{F\in\mathcal{F}_P} \big(\mathcal{N}_T^0 \cup \mathcal{N}_T^1 \cup \mathcal{N}_T^2\big) \cup \mathcal{N}_P \cup \widetilde{\mathcal{N}}_P \tag{4.3}$$

is a nodal minimal determining set for $\mathcal{S}_P$, where

(1) $\mathcal{N}_v := \bigcup_{|\alpha|\leqslant 6}\{\varepsilon_v D^\alpha\}$,
(2) $\mathcal{N}_e := \bigcup_{i=1}^3 \bigcup_{j=1}^i \{\varepsilon_{\eta_{e,j}^i} D_e^\alpha\}_{|\alpha|=i}$,
(3) $\mathcal{N}_F^0 := \{\varepsilon_\xi D_F\}_{\xi\in\mathcal{A}_F^0}$,
(4) $\mathcal{N}_F^1 := \{\varepsilon_\xi D_F\}_{\xi\in\mathcal{A}_F^1}$,
(5) $\mathcal{N}_F^2 := \{\varepsilon_\xi D_F\}_{\xi\in\mathcal{A}_F^2}$,
(6) $\mathcal{N}_P := \bigcup_{|\alpha|\leqslant 6}\{\varepsilon_{O_P} D^\alpha\}$,
(7) $\widetilde{\mathcal{N}}_P := \bigcup_{|\alpha|>6,\|\alpha\|\leqslant 3}\{\varepsilon_{O_P} D^\alpha\}$.

Proof. We first compute the cardinality of $\mathcal{N}$. It is easy to see that the cardinalities of the sets $\mathcal{N}_v, \mathcal{N}_e, \mathcal{N}_F^0, \mathcal{N}_F^1, \mathcal{N}_F^2$, $\mathcal{N}_P, \widetilde{\mathcal{N}}_P$ are 84, 20, 3, 10, 18, 84, and 10. Since P has six vertices, twelve edges, and eight faces, it follows that $\dim \mathcal{S}_P = 84\times 6 + 20\times 12 + 31\times 8 + 94$ if $\mathcal{N}$ is a nodal minimal determining set.

To show that $\mathcal{N}$ is a nodal minimal determining set, we show that setting the values $\{\lambda s\}_{\lambda\in\mathcal{N}}$ of a spline s in $\mathcal{S}_P$ uniquely determines all B-coefficients of s. First, the C^6 smoothness at each $v \in \mathcal{V}_P$ and at O_P implies that setting $\{\lambda s\}_{\lambda\in\{\mathcal{N}_v\cup\mathcal{N}_P\}}$ uniquely determines the B-coefficients corresponding to domain points in the balls $B_6(v)$ and $B_6(O_P)$. Similarly, the $C^3_\otimes$ smoothness at O_P implies that setting $\{\lambda s\}_{\lambda\in\widetilde{\mathcal{N}}_P}$ uniquely determines the B-coefficients corresponding to the remaining domain points in the p-ball $B_{\otimes,3}(O_P)$. Next, the C^3 smoothness around each $e \in \mathcal{E}_P$ shows that setting $\{\lambda s\}_{\lambda\in\mathcal{N}_e}$ uniquely determines the B-coefficients corresponding to the remaining domain points in the tube of radius three around e. From the proof of Theorem 3.1 in (Alfeld and Schumaker, 2005a), it follows that setting $\{\lambda s\}_{\lambda\in\{\mathcal{N}_F^0\cup\mathcal{N}_F^1\cup\mathcal{N}_F^2\}}$ uniquely determines the B-coefficients corresponding to the remaining domain points on $H_{13}(O_P)$, $H_{12}(O_P)$, and $H_{11}(O_P)$, shown as black triangles in Fig. 6. In Fig. 7 all the domain points in $H_{13}(v_1)$ whose coefficients have been defined so far are shown as black dots.

Next, we show that applying the C^3 smoothness across the interior faces of $\triangle_P$ uniquely determines the coefficients corresponding to the remaining domain points in the tubes of radius four around each $e \in \mathcal{E}_P$. These points are located on $H_{10}(O_P)$ and $Fr(H_9(O_P))$, and are depicted as black triangles in Fig. 8. Each of those coefficients is determined by solving a system of three linear equations with three unknowns. This system is associated with a univariate spline

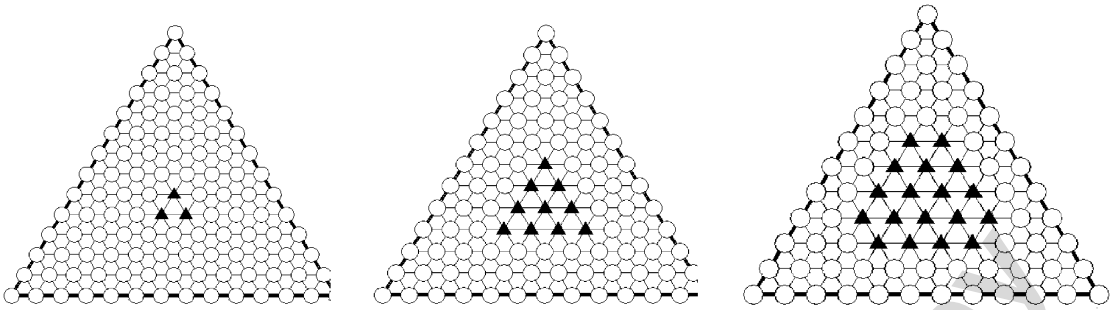

Fig. 6. Black triangles depict domain points whose B-coefficients are determined by the functionals associated with $\mathcal{A}_F^0$, $\mathcal{A}_F^1$, and $\mathcal{A}_F^2$, respectively.

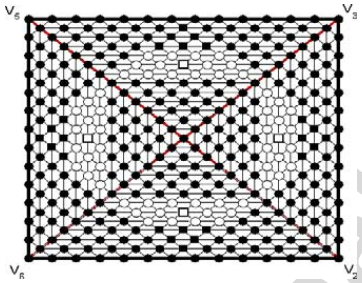

Fig. 7. Domain points on $H_{13}(v_1)$.

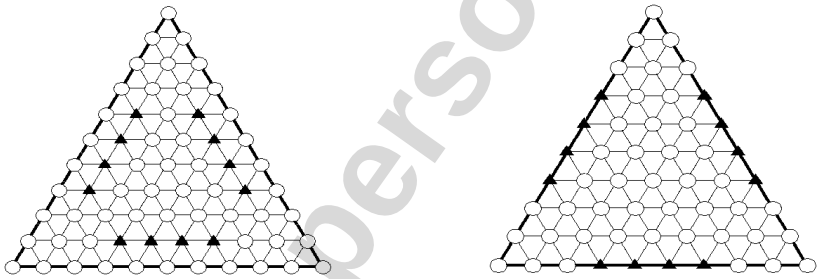

Fig. 8. Black triangles depict domain points on faces of $H_{10}(O_P)$ (left) and $Fr(H_9(O_P))$ (right) whose B-coefficients are determined by the C^3 smoothness across interior faces of P.

in $\mathcal{S}_4^3(\triangle_{[a,b]})$, where $\triangle_{[a,b]}$ is a split of $[a,b]$ into two segments by an arbitrary interior point c. In Fig. 9 (left), we marked the domain points corresponding to the unknown coefficients with open dots, and the domain points whose coefficients have already been determined are depicted as black dots. The open dot at the split point c is actually located on $Fr(H_9(O_P))$, and the black dots at the points a and b are located on $H_{13}(O_P)$. The C^3 smoothness condition leads to a 3×3 matrix that is known to be nonsingular. At this point, the B-coefficients corresponding to all domain points in the tubes of radius four of every $e \in \mathcal{E}_P$ are uniquely determined.

As the next step, we apply the individual C^5 and C^4 smoothness conditions associated with the functionals in $\mathcal{T}_{e,P}$. The points whose coefficients enter those conditions, are located on the intersections of shells of radius nine around two neighboring vertices of P, and are depicted in Fig. 4 (left), where the domain points corresponding to the unknown coefficients are marked as open dots. The complete set of these points is described in Lemma 3.3, where $\mathcal{M}_e^1$ are the domain points whose coefficients have already been determined, and $\mathcal{M}_e^2$ is the set of domain points with unknown coefficients. Each of the unknown coefficients is determined by solving a system of five linear equations with five unknowns. This system is associated with a univariate spline in $\mathcal{S}_5^5(\triangle_{[a,b]})$, where $\triangle_{[a,b]}$ is a split of $[a,b]$ into two segments by an arbitrary interior point c. In Fig. 9 (right), the domain points corresponding to the unknown coefficients are shown as open dots, and the domain points whose coefficients have already been determined are marked as black dots. The open dot at the split point c is actually located on $Fr(H_8(O_P))$, and the black dots at the points a and b are located on $H_{13}(O_P)$. Increasing the smoothness from C^3 to C^4 and C^5, leads to a 5×5 nonsingular matrix, and allows us to determine uniquely the B-coefficients corresponding to the domain points in $\mathcal{M}_e^2$ for every $e \in \mathcal{E}_P$.

Fig. 9. Domain points associated with the C^3 smoothness functionals across interior faces of P (left), and the functionals in $\mathcal{T}_{e,P}$ (right).

With the help of Lemma 3.4, we observe that at this point all still undetermined coefficients correspond to domain points in $H_7(v) \cup H_8(v) \cup H_9(v)$, $v \in \mathcal{V}_P$. According to Lemmas 3.2, and 3.3, the shells of radii seven, eight and nine around the vertices of P intersect at the domain points whose coefficients have already been determined. Therefore, for each v we can consider its shells $H_i(v)$, $i = 7, 8, 9$, in the bivariate setting, independently of the shells of radii seven, eight and nine of the other vertices of P. Applying Lemmas 5.1–5.3 for each $v \in \mathcal{V}_P$, we conclude that the coefficients corresponding to all the remaining domain points are uniquely determined. Therefore, we have established that $\mathcal{N}$ is a nodal minimal determining set for $\mathcal{S}_P$. □

Let $\widetilde{\triangle}$ be an arbitrary octahedral partition of a polygonal domain Ω, and let $\mathcal{V}$, $\mathcal{E}$, and $\mathcal{F}$ be its sets of vertices, edges, and faces, respectively. Having split each octahedron into eight tetrahedra according to Definition 3.1, we obtain a tetrahedralization $\triangle$ of Ω. We now define the space of super-splines on $\triangle$:

$$\begin{aligned}\mathcal{S}(\triangle) := \big\{ s \in C^2(\Omega):\ & s|_T \in \mathcal{P}_{13}^3 \text{ all tetrahedra } T \in \triangle, \\ & s \in C^3(e) \text{ for all } e \in \mathcal{E},\ s \in C^6(v) \text{ for all } v \in \mathcal{V}, \\ & s|_P \in \mathcal{S}_P \text{ for all } P \in \widetilde{\triangle} \big\}, \end{aligned} \tag{4.4}$$

where $\mathcal{S}_P$ is as in (4.2).

Our next theorem shows that the construction in Theorem 4.1 provides a C^2 macro-element space. The proof is omitted since it is very similar to that of Theorem 3.2 in (Alfeld and Schumaker, 2005a).

Theorem 4.2. *The dimension of the space $\mathcal{S}(\triangle)$ is $84V + 20E + 31F + 94N$, where V, E, F, N are the numbers of vertices, edges, faces, and octahedra in $\widetilde{\triangle}$, respectively. Moreover,*

$$\mathcal{N} := \bigcup_{v\in\mathcal{V}} \mathcal{N}_v \cup \bigcup_{e\in\mathcal{E}} \mathcal{N}_e \bigcup_{F\in\mathcal{F}} \big(\mathcal{N}_F^0 \cup \mathcal{N}_F^1 \cup \mathcal{N}_F^2\big) \cup \bigcup_{P\in\triangle} (\mathcal{N}_{O_P} \cup \widetilde{\mathcal{N}}_{O_P}) \tag{4.5}$$

is a nodal minimal determining set for $\mathcal{S}(\triangle)$, where $\mathcal{N}_v, \mathcal{N}_e, \mathcal{N}_F^0, \mathcal{N}_F^1, \mathcal{N}_F^2, \mathcal{N}_{O_P}$, and $\widetilde{\mathcal{N}}_{O_P}$ are as in Theorem 4.1.

Theorem 4.2 shows that for any function $f \in C^9(\Omega)$, there is a unique spline $s_f \in \mathcal{S}(\triangle)$ solving the Hermite interpolation problem

$$\lambda s_f = \lambda f, \quad \text{for all } \lambda \in \mathcal{N},$$

where $\mathcal{N}$ is as in Theorem 4.2. Our next theorem establishes an optimal error bound for the approximation of $f \in C^9(\Omega)$ by $s_f \in \mathcal{S}(\triangle)$. Let P be as in Definition 3.1, and let

$$\delta_P := \min_{i=1,2,3} \min\left\{ \frac{|\langle v_i, O_P\rangle|}{|\langle v_i, v_{i+3}\rangle|}, \frac{|\langle v_{i+3}, O_P\rangle|}{|\langle v_i, v_{i+3}\rangle|} \right\}.$$

Then the coefficients corresponding to the domain points in $\mathcal{D}_{\triangle_P,13}$ which are not in the nodal minimal determining set described in Theorem 4.1, are computed from essentially univariate smoothness conditions. This computation process is known to be dependent on δ_P. The proof of our next theorem is very similar to that of Theorem 3.3 in (Alfeld and Schumaker, 2005a), and, thus, we omit it.

Theorem 4.3. *For all $f \in C^m(\Omega)$ with $9 \leqslant m \leqslant 13$, there exists a constant K depending only on δ and the smallest angle in $\widetilde{\triangle}$, such that for all $|\alpha| \leqslant m$,*

$$\big\| D^\alpha (f - s_f) \big\|_\Omega \leqslant K |\triangle|^{m+1-\alpha} |f|_{m+1,\Omega}, \tag{4.6}$$

where $|\triangle|$ is the maximum diameter of the octahedra in $\widetilde{\triangle}$, $\delta := \min_{P\in\widetilde{\triangle}} \delta_P$, and

$$|f|_{m+1,\Omega} := \sum_{|\alpha|=m+1} \big\| D^\alpha f \big\|_\Omega.$$

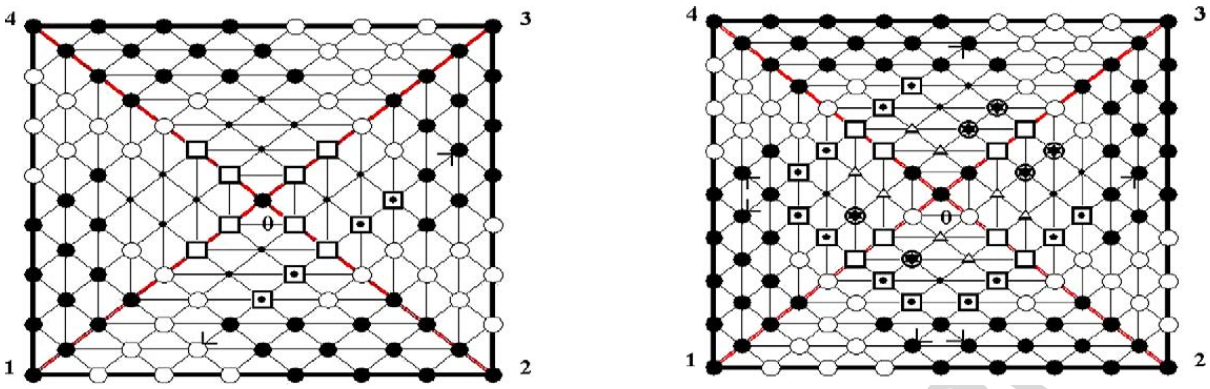

Fig. 10. Domain points on $H_7(v)$ (left), and $H_8(v)$ (right).

5. Some bivariate spline spaces

In this section we prove three lemmas which are needed for the proof of Theorem 4.1. Throughout this section we suppose that $F := \langle u_1, u_2, u_3, u_4\rangle$ is a rectangle which has been split into four triangles by drawing in both diagonals, see the shaded region in Fig. 3 (right). Let $\triangle_F$ be the associated triangulation, and let u_0 be the point where the diagonals of F intersect. Let

$$\begin{aligned}\mathcal{S}_{F,7} := \big\{s \in C^3(F)\colon\ & s|_T \in \mathcal{P}_7^2 \text{ all triangles } T \in \triangle_F,\\ & s \in C^4(u_0),\ \tau_{12}^4 s = 0,\ (u_1, \langle u_0, u_2\rangle, u_3)\big\}.\end{aligned} \tag{5.1}$$

In Fig. 10 (left) the domain points associated with τ_{12}^4 in both triangles sharing the edge $\langle u_0, u_2\rangle$ are located at the tips of the arrows. Let

$$\begin{aligned}\mathcal{S}_{F,8} := \big\{s \in C^3(F)\colon\ & s|_T \in \mathcal{P}_8^2 \text{ all triangles } T \in \triangle_F,\ s \in C^5(u_0),\\ & \tau_{13}^4 s = 0,\ \big(u_1, \langle u_0, u_2\rangle, u_3\big),\\ & \big(u_1, \langle u_0, u_4\rangle, u_3\big),\ \big(u_2, \langle u_0, u_1\rangle, u_4\big)\big\}.\end{aligned} \tag{5.2}$$

In Fig. 10 (right) the domain points associated with each functional τ_{13}^4 in both triangles sharing the edge $\langle u_0, u_i\rangle$ are located at the tips of the arrows. Let

$$\begin{aligned}\mathcal{S}_{F,9} := \big\{s \in C^3(F)\colon\ & s|_T \in \mathcal{P}_9^2 \text{ all triangles } T \in \triangle_F,\ s \in C^4(u_0),\\ & \tau_{i3}^{6-i} s = 0,\ i = 0, 1, 2,\ \big(u_1, \langle u_0, u_2\rangle, u_3\big),\ \big(u_1, \langle u_0, u_4\rangle, u_3\big),\\ & \tau_{i2}^{7-i} s = 0,\ i = 2, 3,\ \big(u_1, \langle u_0, u_2\rangle, u_3\big)\big\}.\end{aligned} \tag{5.3}$$

In Fig. 11 the domain points associated with τ_{i3}^{6-i} in both triangles sharing the edge $\langle u_0, u_2\rangle$ are located at the tips of the arrows on $R_6(u_2)$. The domain points associated with τ_{i3}^{6-i} in both triangles sharing the edge $\langle u_0, u_4\rangle$ are located at the tips of the arrows on $R_6(u_4)$. Finally, the domain points associated with τ_{i2}^{7-i} in both triangles sharing the edge $\langle u_0, u_2\rangle$ are located at the tips of the arrows on $R_7(u_2)$.

Lemma 5.1. *The set $\mathcal{M}_{F,7}$ of fifty-three domain points marked with large black dots in Fig.* 10 (*left*) *is a minimal determining set for $\mathcal{S}_{F,7}$.*

Proof. First we show that $\mathcal{M}_{F,7}$ is a determining set for $\mathcal{S}_{F,7}$. Suppose $g \in \mathcal{S}_{F,7}$ is such that its coefficients corresponding to the points in $\mathcal{M}_{F,7}$ are zero. First, we use the C^3 continuity across the edges $\langle u_0, u_i\rangle$, $i = 1, \ldots, 4$, to show that the coefficients marked with open circles in Fig. 10 (left) are zero. Using the C^4 continuity at u_0 shows that the coefficients corresponding to the points marked with open boxes must be zero. Then by the individual smoothness condition τ_{12}^4 coupled with the C^3 continuity across the edge $\langle u_0, u_2\rangle$, the coefficients corresponding to the points marked with open boxes with a dot also vanish. Finally, using the C^3 smoothness conditions across

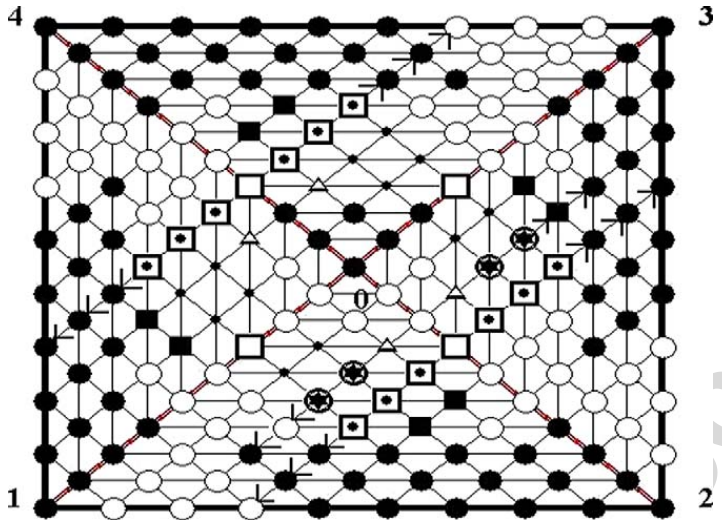

Fig. 11. Domain points on $H_9(v)$.

the edges $\langle u_0, u_1\rangle$, and $\langle u_0, u_3\rangle$, we see that the remaining coefficients corresponding to the twelve domain points marked with small dots must also be zero. This completes the proof that $\mathcal{M}_{F,7}$ is a determining set for $\mathcal{S}_{F,7}$. Since $\dim[\mathcal{S}_7^3(\triangle_F) \cap C^4(u_0)] = 54$ by Theorem 2.2 of (Schumaker, 1988), and we imposed one additional smoothness condition, it follows that $\dim \mathcal{S}_{F,7} \geqslant 53$. The set $\mathcal{M}_{F,7}$ contains exactly fifty-three points. Hence, $\mathcal{M}_{F,7}$ is a MDS for $\mathcal{S}_{F,7}$. □

Lemma 5.2. *The set $\mathcal{M}_{F,8}$ of sixty-seven domain points marked with large black dots in Fig.* 10 (*right*) *is a minimal determining set for $\mathcal{S}_{F,8}$.*

Proof. First we show that $\mathcal{M}_{F,8}$ is a determining set for $\mathcal{S}_{F,8}$. Suppose $g \in \mathcal{S}_{F,8}$ is such that its coefficients corresponding to the points in $\mathcal{M}_{F,8}$ are zero. First, we use the C^3 continuity across the edges $\langle u_0, u_i\rangle$, $i = 1, \ldots, 4$, to show that the coefficients marked with open circles in Fig. 10 (right) are zero. Using the C^5 continuity at u_0 shows that the coefficients corresponding to the points marked with open boxes must be zero. Then, for each $i = 1, 2, 4$, by the individual smoothness condition τ_{13}^4 associated with that edge $\langle u_0, u_i\rangle$ coupled with the C^3 continuity across edge, the coefficients corresponding to the points marked with open boxes with a dot and located on $R_5(u_i)$, $i = 1, 2, 4$, vanish. Then applying the C^5 continuity at u_0 across $\langle u_0, u_1\rangle$ and $\langle u_0, u_3\rangle$, shows that the eight coefficients corresponding to the points marked with open triangles are all zero. By the C^5 continuity at u_0 across $\langle u_0, u_2\rangle$ and $\langle u_0, u_4\rangle$, the six coefficients corresponding to the points marked as open circles with a star vanish. Finally, using the C^3 smoothness conditions across the edges $\langle u_0, u_1\rangle$ and $\langle u_0, u_3\rangle$, we see that the remaining coefficients corresponding to the six domain points marked with small dots must also be zero. This completes the proof that $\mathcal{M}_{F,8}$ is a determining set for $\mathcal{S}_{F,7}$. Since $\dim[\mathcal{S}_8^3(\triangle_F) \cap C^5(u_0)] = 70$ by Theorem 2.2 of (Schumaker, 1988), and we imposed three additional smoothness conditions, it follows that $\dim \mathcal{S}_{F,8} \geqslant 67$. The set $\mathcal{M}_{F,8}$ contains exactly sixty-seven points. Hence, $\mathcal{M}_{F,8}$ is a MDS for $\mathcal{S}_{F,8}$. □

Lemma 5.3. *The set $\mathcal{M}_{F,9}$ of ninety domain points marked with large black dots and black boxes in Fig.* 11 *is a minimal determining set for $\mathcal{S}_{F,9}$.*

Proof. To show that $\mathcal{M}_{F,9}$ is a determining set for $\mathcal{S}_{F,9}$, suppose $g \in \mathcal{S}_{F,9}$ is such that its coefficients corresponding to the points in $\mathcal{M}_{F,9}$ are zero. First, using the C^3 continuity across the edges $\langle u_0, u_i\rangle$, $i = 1, \ldots, 4$, shows that the coefficients marked with open circles in Fig. 11 are zero. Using the C^4 continuity at u_0 shows that the coefficients corresponding to the points marked with open boxes must also be zero. Then, for each $i = 0, 1, 2$, using the individual smoothness conditions τ_{i3}^{6-i}, associated with the edge $\langle u_0, u_i\rangle$, $i = 2, 4$, coupled with the C^3 continuity across that edge, the coefficients corresponding to the points marked with open boxes with a dot and located on $R_5(u_i)$, $i = 2, 4$, vanish. Then applying C^3 continuity across the edges $\langle u_0, u_1\rangle$, and $\langle u_0, u_3\rangle$ shows that the four coefficients corresponding to the points marked with open triangles are all zero. Next, using the individual smoothness conditions

τ_{i2}^{7-i}, $i = 2, 3$, associated with the edge $\langle u_0, u_2\rangle$ together with the C^3 continuity across the same edge, the coefficients corresponding to the points marked with circles containing a star and located on $R_7(u_2)$ vanish. Finally, using the C^3 smoothness conditions across the edges $\langle u_0, u_1\rangle$, and $\langle u_0, u_3\rangle$ we see that the remaining coefficients corresponding to the twelve domain points marked with small dots must also be zero. This completes the proof that $\mathcal{M}_{F,9}$ is a determining set for $\mathcal{S}_{F,9}$. Since $\dim[\mathcal{S}_9^3(\triangle_F) \cap C^4(u_0)] = 98$ by Theorem 2.2 of (Schumaker, 1988), and we imposed eight additional smoothness conditions, it follows that $\dim \mathcal{S}_{F,9} \geqslant 90$. The set $\mathcal{M}_{F,9}$ contains exactly ninety points, and therefore, it forms a MDS for $\mathcal{S}_{F,9}$. □

6. Remarks

Remark 6.1. Bivariate C^r macro-elements have been extensively studied by a number of authors, see e.g. (Alfeld and Schumaker, 2002a, 2002b; Lai and Schumaker, 2001, 2003; Ženišek, 1974).

Remark 6.2. C^1 and C^2 trivariate macro-elements defined on nonsplit tetrahedra were studied in (Le Méhauté, 1984). They use polynomial splines of degree nine and seventeen, respectively.

Remark 6.3. Let $x_1 < \cdots < x_n$, $y_1 < \cdots < y_m$, $z_1 < \cdots < z_l$ be sets of n, m, and l points in $\mathbb{R}$, respectively, and

$$V := \{v_{ijk} = (x_i, y_j, z_k),\ i = 1, \ldots, n,\ j = 1, \ldots, m,\ k = 1, \ldots, l\},$$

be the set of $n \times m \times l$ points in the domain $\Omega := [x_1, x_n] \times [y_1, y_m] \times [z_1, z_l]$. The collection of boxes $Q_{ijk} = [x_i, x_{i+1}] \times [y_j, y_{j+1}] \times [z_k, z_{k+1}]$, where $i = 1, \ldots, n-1$, $j = 1, \ldots, m-1$, forms a partition $\triangle_1$ of Ω. Then we split each Q_{ijk} into twenty-four tetrahedra. First, we draw in the diagonals of each rectangular face, and thus obtain the centers of the six faces, see Fig. 12 (left). Then we connect the center of Q_{ijk} (the intersection of the main diagonals of the box) with each vertex of Q_{ijk}, and with the six centers of the faces. The new partition $\triangle$ of Ω (C^1 splines on such partitions were extensively studied in (Hangelbroek et al., 2004) and (Schumaker and Sorokina, 2005)) allows us to use the octahedral C^2 macro-element constructed in Section 4. Indeed, let Q_{ijk} be as in Fig. 12 (left), and $Q_{i+1,j,k}$ be its neighbor on the right, sharing the face $\langle 2, 3, 6, 5\rangle$. Then the octahedron whose vertices are the centers of Q_{ijk} and $Q_{i+1,j,k}$, and the four vertices forming $\langle 2, 3, 6, 5\rangle$, is split into eight tetrahedra, as required for our scheme. The boundary of Ω needs a special treatment, because instead of an octahedron we have to deal with a half of it – a pyramid. Suppose u is the interior vertex of such a pyramid, and v_1, v_2, v_3, v_4 are boundary vertices. Then we apply the scheme described in Section 4 to shells of radius seven, eight and nine of u. Additionally, we have to consider $H_i(u)$ for $i = 10, \ldots, 13$. Each of these shells forms a set of domain points for a bivariate spline of degree i and smoothness three. Therefore, it can be treated separately and similarly to the super-spline spaces described in Section 5.

Remark 6.4. Let $\triangle_1$ be as in Remark 6.3, and n, m, l be even. Let

$$V_b := \{v_{ijk} \in V\colon\ i + j + k \text{ is even}\},$$
$$V_w := \{v_{ijk} \in V\colon\ i + j + k \text{ is odd}\}.$$

Then each box Q_{ijk} has four vertices in V_b, and the other four in V_w. We split each Q_{ijk} into five tetrahedra as in Fig. 12 (middle), where the vertices from V_b are shown as black dots, and the vertices from V_w are marked as open dots. The new partition $\triangle$ of Ω (first described in (Schumaker and Sorokina, 2004), where it was called a type-4

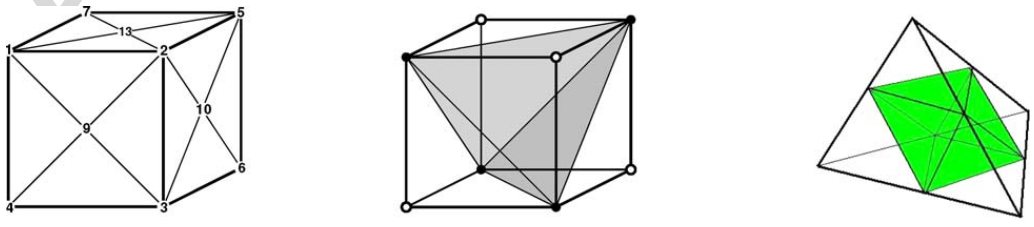

Fig. 12. Two splits of a box and a refinement of a tetrahedron allowing the use of the octahedral macro-element.

tetrahedral partition) allows us to use a combination of the octahedral C^2 macro-element constructed in Section 4, and the 3D Clough–Toucher macro-element constructed in (Alfeld and Schumaker, 2005a). Indeed, let Q_{ijk} be as in Fig. 12 (middle), with $v_{ijk} \in V_w$ being its front-left-lower corner. Then the shaded tetrahedron in Q_{ijk} whose vertices are in V_b, and are marked as black dots, can be treated according to the 3D Clough–Toucher scheme. On the other hand, v_{ijk} is shared by eight boxes. The set of six vertices

$$\{v_{i-1,j,k}, v_{i,j-1,k}, v_{i,j,k-1}, v_{i+1,j,k}, v_{i,j+1,k}, v_{i,j,k+1}\} \subset V_b,$$

forms an octahedron, which is split into eight tetrahedra using its center—v_{ijk}. The boundary of Ω needs a special treatment. The easiest way to deal with is to apply the 3D Clough–Toucher scheme to each boundary tetrahedron.

Remark 6.5. Let $T := \langle v_1, v_2, v_3, v_4\rangle$ be a tetrahedron, and let

$$U_T := \big\{u_{ij} := (v_i + v_j)/2,\ (ij) \in \big\{(12), (13), (14), (23), (24), (34)\big\}\big\}$$

be the set of midpoints of six edges of T. It is easy to see that U_T forms a set of vertices of an octahedron P_T. Drawing in the line segments connecting the midpoints of the edges lying on the same face of T, we obtain the partition of T into four subtetrahedra, and one octahedron P_T whose vertices are the points in U_T, see Fig. 12 (right). Now we can use the 3D Clough–Toucher scheme on each of the four subtetrahedra, and the octahedral macro-element on P_T. This partition was thoroughly studied in (Ong, 1994), where it was shown that this type of refinement of T does not yield smaller angles, and thus, see Theorem 4.3, does not influence stability.

Remark 6.6. We constructed our octahedral macro-element with as much similarity to the 3D Clough–Tocher one in (Alfeld and Schumaker, 2005a) as possible to facilitate their joint usage, see Remark 6.4. We use the same nodal functionals on the triangular faces of an octahedron as in (Alfeld and Schumaker, 2005a). However, there are differences in smoothness conditions across interior faces. In particular, in the 3D Clough–Toucher scheme there are four tetrahedra meeting at the center. In our scheme we have eight tetrahedra sharing the interior vertex. Due to this fact, for the octahedral macro-element it is impossible to set stronger smoothness conditions at the center, as it is was done in (Alfeld and Schumaker, 2005a).

Remark 6.7. The construction of the macro-element described in this paper is not unique in the sense that there are other choices of the extra smoothness conditions which also lead to macro-elements based on the degrees of freedom used here. It is also possible to use different nodal functionals inside of an octahedron.

Remark 6.8. The use of $C^r_\otimes$ smoothness seems natural for the family of C^r octahedral macro-elements. In particular, for the C^1 octahedral macro-element constructed in (Lai and Le Méhauté, 2004), it is possible to apply $C^1_\otimes$ at the center O_P of the octahedron, and set $\{\varepsilon_{O_P} D^\alpha\}_{\|\alpha\|\leqslant 1}$. This leads to the simplest and most elegant construction.

Remark 6.9. In analyzing the bivariate super-spline spaces of Section 4, we have used the java code developed by Alfeld (www.math.utah.edu/~alfeld), and described in (Alfeld, 2000).

References

Alfeld, P., 2000. Bivariate splines and minimal determining sets. J. Comput. Appl. Math. 119, 13–27.

Alfeld, P., Schumaker, L.L., 2002a. Smooth macro-elements based on Clough–Tocher triangle splits. Numer. Math. 90, 597–616.

Alfeld, P., Schumaker, L.L., 2002b. Smooth macro-elements based on Powell–Sabin triangle splits. Adv. Comp. Math. 16, 29–46.

Alfeld, P., Schumaker, L.L., 2005a. A C^2 trivariate macro-element based on the Clough–Toucher split of a tetrahedron. Computer Aided Geometric Design 22, 710–721.

Alfeld, P., Schumaker, L.L., 2005b. A C^2 trivariate macro-element based on the Worsey–Farin split of a tetrahedron. SIAM J. Numer. Anal. 43, 1750–1765.

Hangelbroek, T., Nürnberger, G., Rössl, C., Zeilfelder, F., 2004. Dimension of C^1 splines on type-6 tetrahedral partitions. J. Approx. Theory 131, 157–184.

Lai, M.-J., Le Méhauté, A., 2004. A new kind of trivariate C^1 spline. Adv. Comp. Math. 21, 273–292.

Lai, M.-J., Schumaker, L.L., 2001. Macro-elements and stable local bases for splines on Clough–Tocher triangulations. Numer. Math. 88, 105–119.

Lai, M.-J., Schumaker, L.L., 2003. Macro-elements and stable local bases for splines on Powell–Sabin triangulations. Math. Comp. 72, 335–354.

Le Méhauté, A., 1984. Interpolation et approximation par des fonctions polynomiales par morceaux dans $\mathbb{R}^n$. Dissertation, L'Universite de Rennes, France.
Ong, M.E.G., 1994. Uniform refinement of a tetrahedron. SIAM J. Sci. Comput. 15, 1134–1145.
Schumaker, L.L., 1988. Dual bases for spline spaces on cells. Computer Aided Geometric Design 5, 277–284.
Schumaker, L.L., Sorokina, T., 2004. C^1 quintic splines on type-4 tetrahedral partitions. Adv. Comp. Math. 21, 421–444.
Schumaker, L.L., Sorokina, T., 2005. A trivariate box macro-element. Constr. Approx. 21, 413–431.
Ženišek, A., 1974. A general theorem on triangular C^m elements. Rev. Francaise Automat. Informat. Rech. Opér., Anal. Numer. 22, 119–127.